In Vivo, in Vitro, and Calculated Vibrational Spectra of Plastoquinone and the Plastosemiquinone Anion Radical

M. Reza Razeghifard,[†] Sunyoung Kim,[†] Jason S. Patzlaff,[†] Ronald S. Hutchison,[†] Thomas Krick,[†] Idelisa Ayala,[†] Jacqueline J. Steenhuis,[†,‡] Scott E. Boesch,[§] Ralph A. Wheeler,*[,§] and Bridgette A. Barry*[,†]

Department of Biochemistry, Molecular Biology and Biophysics, University of Minnesota, St. Paul, Minnesota 55108, and Department of Chemistry and Biochemistry, University of Oklahoma, Norman, Oklahoma 73019

Received: June 14, 1999; In Final Form: August 27, 1999

Plastoquinone (PQ-9) is active as an electron/proton transfer component in photosynthetic membranes. For example, in the photosynthetic complex, photosystem II (PSII), PQ-9 acts as Q_A, a one-electron acceptor, and as Q_B, a two electron, two proton accepting species. Light-minus-dark difference Fourier transform infrared (FT-IR) spectroscopy is a technique with which mechanistic information can be obtained concerning PSII. Here, we present combined experimental and computational studies designed to identify the vibrational contributions of the electron acceptor, Q_A, in its oxidized and one-electron reduced states to the difference FT-IR spectrum. Infrared spectra of decyl-PQ and PQ-9 were obtained; the difference infrared spectra associated with the formation of the corresponding anion radicals were also generated in ethanol solutions. Vibrational mode assignments were made based on hybrid Hartree−Fock/density functional (HF/DF) B3LYP calculations with a 6-31G(d) basis set. Calculations were performed for hydrogen bonded models of PQ-1 and its radical anion. In addition, a methionine-tolerant strain of the cyanobacterium, *Synechocystis sp*. PCC 6803, was used to deuterate PQ-9 in PSII. The macrocycle and phytol tail of chlorophyll were not labeled by this procedure. Mass spectral data may be consistent with partial 13^3 methoxy labeling of chlorophyll. Lack of phytol labeling implies that carotenoids were unlabeled. Difference FT-IR spectra were then obtained by illumination at 80 K, resulting in the one-electron reduction of Q_A. When spectra were obtained of PSII preparations, in which 39% of PQ was $^2H_3$ labeled and 48% was $^2H_6$ labeled, isotope-induced shifts were observed. Comparison of these data to vibrational spectra obtained in vitro and to mode frequencies and intensities from B3LYP/6-31G(d) calculations provides the basis for vibrational mode assignments.

Photosystem II (PSII), a membrane-associated pigment−protein complex, carries out the oxidation of water and reduction of PQ-9 (plastoquinone-9) in all oxygen-evolving plants, algae, and cyanobacteria. Photoexcitation of the primary electron donor, P_{680}, results in electron transfer to a bound PQ-9, called Q_A, via a pheophytin molecule. Reduced Q_A is reoxidized by an exchangeable PQ-9, named Q_B. Q_A functions as a one-electron acceptor, and the reduced form, Q_A^-, is an unprotonated semiquinone anion radical. Q_B, on the other hand, is a two-electron, two-proton acceptor {reviewed in ref 1}. Electron transfer events on the acceptor side of PSII resemble reactions occurring on the acceptor side of the photosynthetic bacterial reaction center.[2] This enzyme, for which high-resolution structural information is available, uses UQ (ubiquinone) or menaquinone, instead of PQ-9, as acceptor molecules {reviewed in ref 3}.

On the donor side of PSII, P_{680}^+ is reduced by a redox-active tyrosine, Z.[4−8] The tyrosine radical, Z$^\bullet$, is reduced by a multinuclear manganese cluster on the microsecond to millisecond time range {see ref 9 and references therein}. Four sequential oxidations of the PSII active site are required for catalysis; the oxidation states of the manganese cluster are called S_i states, where *i* represents the number of oxidative equivalents accumulated.[10] When electron donation from the catalytic site is blocked, the high potential form of cytochrome b-559 or a chlorophyll (chl) molecule, chl_Z, can act as an electron donor.[11,12] PSII also contains two other redox-active tyrosines, D[13] and M;[14] the functional roles of these species in water oxidation have not as yet been elucidated.[15] The bacterial reaction center, which is not capable of water oxidation, does not contain redox-active tyrosines or a manganese cluster, but is predicted to exhibit some structural similarity to PSII.[16,17]

In this report, light-minus-dark FT-IR (Fourier transform infrared) spectroscopy has been applied to PSII. With this technique, the vibrational spectrum associated with the oxidation and reduction of electron transfer components can be recorded. Contributions to the spectrum from species which do not undergo a functionally important structural change are canceled in the difference spectrum. The advantage of difference FT-IR spectroscopy is the ability to obtain information about dynamic structural changes, and thus mechanism, in enzymes. The assignment of complex difference spectra necessitates the use of a battery of techniques, including isotopic labeling (for review, see refs 18 and 19).

* To whom correspondence should be addressed. (Prof. B. A. Barry) Phone: 612-624-6732. Fax: 612-625-5780. E-mail: barry@biosci.cbs.umn.edu. (Prof. R. A. Wheeler) Phone: 405-325-3502. Fax: 405-325-6111. E-mail: rawheeler@chemdept.chem.ou.edu.

† University of Minnesota.

‡ Present address: Howard Hughes Medical Institute, Stanford Medical School, Stanford, California 94305.

§ University of Oklahoma.

10.1021/jp991942x CCC: $18.00
Published on Web 10/16/1999

The focus of this study is the identification and analysis of the vibrational spectrum associated with the reduction of Q_A in PSII and the reduction of PQ-9 in vitro. In the bacterial reaction center, the difference FT-IR spectrum associated with the reduction of the analogous quinone acceptor, Q_A, has been obtained {for example, see ref 20}. UV resonance Raman spectroscopy has also been used to obtain the vibrational spectrum of Q_A^- in the bacterial reaction center.[21] Key to the success of both these techniques has been the use of isotopic labeling in order to assign the spectrum.[21,22] In the bacterial reaction center, isotopic labeling of Q_A can be achieved by replacement of UQ with isotopically labeled compounds.[23] The reaction center is first depleted of UQ, and the new isotopomer of UQ is then reconstituted.[23] FT-IR and Raman spectroscopies have also been used to characterize redox states of model quinones in vitro; [21,24,25] these data can then be used to interpret the biological spectra.

In PSII, there has been no report of the successful removal and subsequent reconstitution of Q_A in PSII preparations, which are active in oxygen evolution.[26,27] As another approach, we have employed a strategy in which PQ is labeled in situ.[13] To achieve the in situ deuteration of PQ, a methionine-tolerant strain of a cyanobacterium, *Synechocystis* sp. PCC 6803, was derived. PSII can be purified in a functionally active form from this organism,[28] and we show here that growth of this strain on $^2H_3$-methionine results in deuteration of PQ. This is based on the biosynthetic derivation of PQ methyl groups from methionine.[13]

Using this approach, we present the first isotope-based identification of the vibrational lines of Q_A and Q_A^- in PSII. For comparison, we also present the first report of the vibrational spectrum associated with the one-electron reduction of decyl PQ and PQ-9, obtained in vitro. On the basis of density functional calculations, vibrational assignments are proposed.[29]

Materials and Methods

A methionine-tolerant strain of *Synechocystis* 6803 was grown photoautotrophically under sterile conditions in BG-11 medium.[30] Solid BG-11 media contained ultrapure agar, 90 μM L-methionine, and 5 mM TES (*N*-tris(hydroxymethyl)methyl-2-aminoethanesulfonic acid)−NaOH, pH 8.0. The liquid medium was supplemented with either 200 μM L-methionine or 200 μM $^2H_3$-methionine ($C^2H_3SC^1H_2C^1H_2C^1H(N^1H_2)COO^1H$, 98% ^2H; Isotec, Miamisburg, OH). Sterile-filtered methionine was added to the medium from a stock buffered with 50 mM TES−NaOH, pH 8.0. Cultures were harvested after 10 days, and cyanobacterial membranes and PSII particles were purified by protocols previously described.[28,30] Chl and oxygen evolution assays were performed as described previously.[30] The yield of PSII from these cultures was low; more than 400 L of cyanobacterial cells were used for these studies.

Difference FT-IR spectra of PSII particles were recorded on a Nicolet (Madison, WI) 60-SXR spectrometer, which was equipped with a Hansen (R. G. Hansen & Associates, Santa Barbara, CA) liquid nitrogen cryostat and a MCT-B detector, as previously described.[31−33] Spectral conditions were as follows: 4 cm^{-1} resolution; 2.5 cm/s mirror velocity; Happ−Genzel apodization function; 80 K temperature; three levels of zero-filling; 7.5 min data acquisition time. Samples contained 1 molar equivalent of potassium ferricyanide per mole of PSII reaction center.[31−34]

Decyl-PQ was purchased from Sigma, with a stated purity of 75% (St. Louis, MO); PQ-9 was a generous gift from Hoffman-LaRoche (Nutley, NJ). Chl and PQ-9 were also extracted from cyanobacterial membranes and were purified as described previously.[34] The purity and concentration of extracted PQ-9 were determined from the UV spectrum, obtained through the use of a Hitachi U-3000 spectrophotometer (Hitachi Ltd., Tokyo, Japan).

Plasma desorption mass spectrometry was used to determine the extent of labeling in chl and PQ-9.[34] These data were obtained through the use of BIO-ION-20R mass spectrometer (BIO ION, Uppsala, Sweden). The molecular mass of PQ-9 was also determined by electrospray mass spectrometry in the negative ion mode. These data were obtained through the use of Finnigan MAT LCQ mass spectrometer (San Jose, CA).

Infrared spectra were obtained from 23 mM ethanol solutions of decyl-PQ (Sigma, St. Louis, MO) and from 5 mM ethanol solutions of PQ-9 (Hoffman-LaRoche). Data were recorded through the use of a Magna 550 II spectrometer (Nicolet, Madison, WI), equipped with a KBr beam splitter, a MCT/A detector, and a Spectra-Tech microcircle cell, containing a ZnSe crystal (Stamford, CT). A Happ-Genzel apodization function, 4 cm^{-1} resolution, room temperature, and one level of zero filling were employed. A spectrum of ethanol was subtracted through the use of a subtraction parameter of 1.0.

Transient FT-IR spectra, associated with the reduction of PQ in vitro, were obtained through the use of a Magna 550 II spectrometer, equipped with a KBr beam splitter, a MCT/A detector, and a Spectra-Tech microcircle cell. A Happ-Genzel apodization function, 8 cm^{-1} resolution, room temperature, and one level of zero filling were employed. Transient UV−visible absorption spectra, associated with the reduction of PQ in vitro, were also obtained through the use of a diode array equipped 8452A spectrophotometer (Hewlett-Packard, Naperville, IL) at 2 nm resolution. Both FT-IR and UV−vis spectra were recorded at room temperature and were obtained on PQ-9 (Hoffman-LaRoche) and decyl-PQ (Sigma) in ethanol solutions. The semiquinone anion radical was transiently generated by injecting a reductant solution, containing sodium hydroxide, sodium borohydride, and dithionite into the solution of the neutral quinone.[35] For the FT-IR experiment, multiple 60 s scans were collected before the addition of the reductant solution. Sequential 60 s scans were performed after addition in order to follow the time dependence of the FT-IR spectrum. The difference FT-IR spectrum, associated with the one-electron reduction of the quinone, was constructed by subtracting data obtained *before* addition of reductant from data obtained *after* addition of reductant. On each day of data acquisition, transient FT-IR data were also acquired in the above manner from FT-IR samples containing only solvent. These data were used to subtract any vibrational contributions of reductant or of solvent from the FT-IR difference spectrum. Experiments were performed in the same manner for the UV−vis experiments, except that 20 s scans were recorded.

The B3LYP hybrid Hartree−Fock density functional (HF/DF) method[36] was used to calculate the vibrational frequencies of a model for plastoquinone-1 and its radical anion. The B3LYP method was chosen because it is known to give harmonic vibrational frequencies within approximately 4% of experiment, for approximately the same computer time investment as a Hartree−Fock calculation where estimated frequencies vary from experiment by more than 10%.[37] The three-parameter B3LYP method uses a weighted sum of Hartree−Fock (E_X^{HF}), local DF (E_X^{Slater}), and gradient-corrected DF expressions for the exchange and correlation energies as in the following equation:

$$E = aE_X^{Slater} + (1-a)E_X^{HF} + b\Delta E_X^{Becke} + cE_C^{LYP} + (1-c)E_C^{VWN}$$

where (E_X^{Slater}) is Slater's local spin density functional for exchange,[38] E_X^{Becke} is Becke's gradient corrected exchange functional,[39] E_C^{VWN} is the local density correlation functional of Vosko, Wilk, and Nusair,[40] and E_C^{LYP} is the gradient-corrected correlation functional of Lee, Yang, and Parr.[41] Coefficients giving the relative weights of various approximations for the exchange and correlation energies in this method were optimized to reproduce thermochemical data for a variety of small molecules.[36] All calculations reported here were performed using the 6-31G(d) split-valence plus polarization basis set.[42,43] This basis set was chosen because it reproduces the properties of medium-sized organic molecules, including a variety of *p*-benzoquinones and their radical anions,[29,44−48] and is small enough for rapid calculations.

The quantum chemistry programs GAUSSIAN94[49] and GAUSSIAN98[50] were used for all calculations. Berny's optimization algorithm[51] was used to perform full geometry optimizations in C_1 symmetry using internal coordinates. Frequency calculations were performed for the optimized geometries. Because the B3LYP method is well-known to overestimate high frequencies and underestimate low frequencies of vibration, all frequencies presented here were multiplied by 0.9614 for modes appearing at frequencies greater than 1000 cm^{-1} and by 1.0013 for frequencies less than 1000 cm^{-1}.[37] Scaling uniformly shifts all modes above 1000 cm^{-1} to lower frequencies, when compared to frequencies reported in published work where no scaling was employed.[29]

Vibrational mode assignments were performed by calculating total energy distributions using the GAMESS[52,53] quantum chemistry programs, animating each mode using the program XMOL,[54] and comparing the modes of one molecule to another using the progam ViPA, an acronym for vibrational projection analysis.[55,56] The ViPA program[55,56] exploits the vector properties of vibrational normal modes to assess the similarity between modes of an object molecule and a structurally similar basis molecule. The program first aligns the two molecules and calculates each molecule's normal modes and vibrational frequencies. For each molecule, each of the normal vibrational modes is a column vector which is orthonormal to all other normal modes of the same molecule. The vector projection operation is done by sequentially projecting each normal mode of the object molecule onto each normal mode of the basis molecule. The result is a matrix whose elements measure the similarity of a given mode of the object molecule to the modes of the basis molecule. The similarity of any mode of the object molecule to any mode of the basis molecule can then be expressed as a percentage by calculating the sum of the squares of the matrix elements and multiplying by 100. Although vibrational projection analysis has been exploited to compare normal modes modified by isotopic substitution, oxidation/reduction, or covalent modifications,[56,57] the current work presents the first application of vibrational projection analysis to compare a molecule's normal modes with modes perturbed by noncovalent contacts. The structural model for plastoquinone-1 used here is described in previously published work[29] and has terminal methyl groups of the isoprenyl chain replaced by hydrogen atoms. Calculations reported here differ from published work because the current calculations were conducted with one water molecule positioned near the quinone oxygen atoms to model hydrogen bonding. Vibrational projection analysis shows that mode assignments are the same, whether or not hydrogen bonding to PQ oxygens was included in the model.[29]

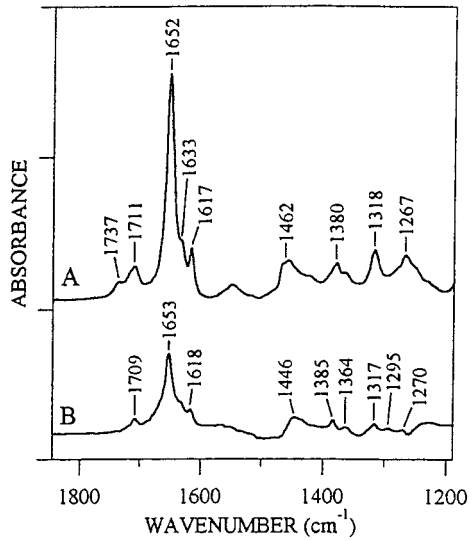

Figure 1. FT-IR spectrum of 23 mM decyl PQ (A) and 5 mM PQ-9 (B). Solvent (ethanol) contributions have been subtracted; spectral conditions are described in Materials and Methods. The tick marks on the *y* axis are 1×10^{-2} absorbance units.

Isotopic substitution calculations were also performed for both PQ-1 and its radical anion in several different ways. First, both methyl groups on the quinone ring were completely deuterated in order to estimate the maximum isotopic frequency shifts. Second, only the methyl group meta or para to the isoprenoid chain was deuterated. Third, two hydrogens in one methyl group and one hydrogen in the other methyl group were deuterated. Vibrational modes for each isotopically substituted species were matched with those of the undeuterated structure by using vibrational projection analysis. In each test, isotopic frequency shifts were very small for the modes of primary interest. Therefore, we discuss only calculations with complete methyl deuteration, where the maximum isotopic shifts are expected.

Results

In Vitro Studies of Decyl-PQ and PQ-9. In Figure 1, we present FT-IR data obtained on decyl-PQ and PQ-9 in vitro. The spectrum of decyl-PQ (Figure 1A) had three bands at 1652, 1633 (shoulder), and 1617 cm^{-1} that were attributable to vibrational modes of the quinonoid ring. This was confirmed by spectra obtained on PQ-9 (Figure 1B), because features at 1653 and 1618 cm^{-1} were also observed in this spectrum. Ring stretching modes and CO stretching modes are expected;[29] the assignment of these vibrational modes will be discussed in more detail below. These spectra exhibited low intensity bands at 1737 (Figure 1A), 1711 (Figure 1A), and 1709 cm^{-1} (Figure 1B). Because fundamental vibrations of decyl PQ and PQ-9 are not expected in this region, these lines are attributable either to a sample contaminant or to a combination band arising from the neutral quinone; combination bands have been observed and assigned previously in the spectrum of 1,4 benzoquinone {see ref 58 and references therein}. Finally, spectral features of low to moderate intensity were observed between 1462 and 1267 cm^{-1} (parts A and B of Figure 1). Lines in this spectral region are attributable to C−H bending modes of the methyl groups, decyl and/or isoprenyl moieties, ring stretches/bends, chain stretches, and ring-chain stretching motions.[29] Significant contributions in this region from the decyl and isoprenoid substituents were confirmed by comparison of parts A and B of Figure 1.

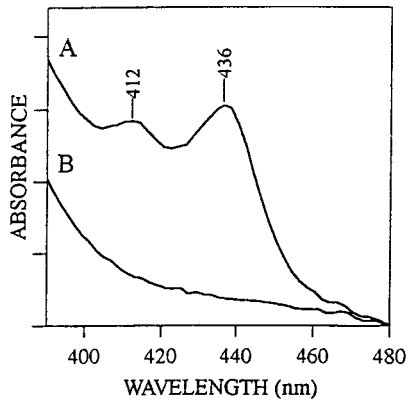

Figure 2. Visible absorption spectrum associated with the one-electron reduction of PQ-9 in vitro. Spectra were obtained 1.7−4.0 min after (A) and before (B) the addition of an alkaline reductant mixture to 0.75 mM PQ-9 in ethanol. The tick marks on the *y* axis correspond to 5×10^{-2} absorbance units. See Materials and Methods for additional experimental details.

Transient absorption spectra, associated with the reduction of PQ-9 in vitro, were also obtained (Figure 2). The addition of electron donors under alkaline conditions in ethanol is expected to generate the neutral semiquinone radical.[35] To identify the time regime in which the semiquinone radical was produced in our experiments, the UV and visible spectra were monitored as a function of time after the addition of reductants to a basic PQ-9 solution. The visible spectrum of the anion radical, arising from a n−π* transition, is unique and distinguishes this species from the neutral PQH• radical and other electron transfer intermediates.[59] As expected, the characteristic spectrum of the PQ-9 anion radical, with peaks at 412 and 436 nm,[35,59] was observed for several minutes after reductant addition. In particular, data obtained 1.7−2.0 min after addition of reductant showed this spectrum. The spectrum was essentially unchanged 2.7−3.0 min after reductant addition (data not shown) and was not observed, as expected, before reductant addition (Figure 2B). Therefore, vibrational data acquired 2−4 min after reductant addition reflect the production of the semiquinone anion radical (Figure 2A).

Accordingly, infrared data were acquired in vitro as a function of time before and 2−3 min after addition of reductant. Difference spectra obtained on decyl PQ are presented in Figure 3A (solid line). As a control, data were also generated using the same procedure, but in the absence of decyl PQ (Figure 3A, dotted line). Such a negative control, showing the effects of addition of reductant on the ethanol solvent (Figure 3A, dotted line), was subtracted from data obtained on decyl PQ in ethanol (Figure 3A, solid line) to construct the difference spectrum associated with the one-electron reduction of decyl PQ (Figure 3B, solid line). This spectrum (Figure 3B, solid line) should have no substantial ethanol contribution. As expected, similar manipulations, using data recorded before reductant addition, gave a flat baseline (Figure 3B, dotted line).

As shown in Figure 3B (solid line), reduction to form the semiquinone anion radical led to dramatic alteration in the vibrational spectrum of decyl PQ. Unique vibrational modes of the anion radical are positive lines in this difference spectrum; unique vibrational modes of neutral decyl-PQ are negative lines. In Figure 3B, an intense negative line was observed at 1653 cm^{-1}; this line was accompanied by shoulders at 1633 and 1618 cm^{-1}. These negative lines had frequencies identical to spectral features observed in Figure 1A; these lines are assignable to the quinone form of decyl PQ. In Figure 3B, positive lines were observed at 1474, 1418, and 1337 cm^{-1}. These lines can be

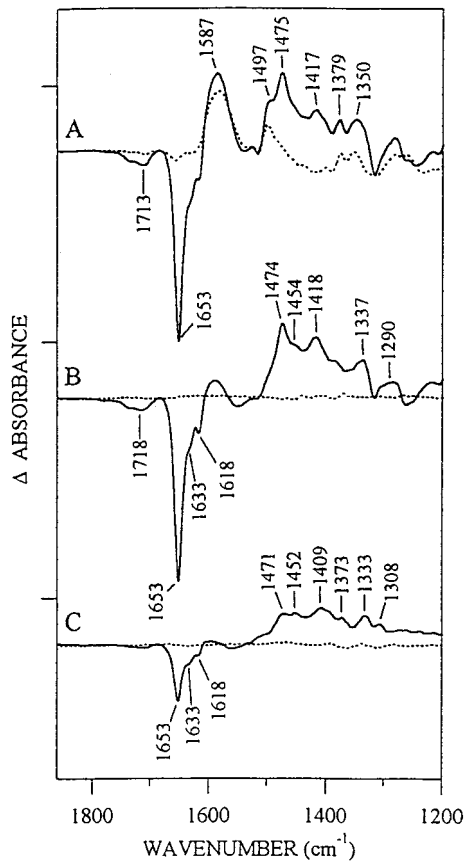

Figure 3. Difference FT-IR spectrum associated with the one-electron reduction of decyl PQ and PQ-9 in vitro. Data were obtained before and 2−3 min after the addition of reductant. In (A), the solid line shows the difference spectrum associated with the addition of an alkaline reductant mixture to 23 mM decyl PQ in ethanol, and the dotted line shows the spectrum obtained when the alkaline reductant mixture is added to ethanol alone. (B, solid line) shows the results of a 1:1 subtraction (solid line in (A) minus dotted line in (A)) and corresponds to the decyl PQ^--minus-decyl PQ difference FT-IR spectrum, with no ethanol contribution. Data recorded *before* the addition of reductant were manipulated in the same manner as a negative control (B, dotted line). (C, solid line) shows the $PQ\text{-}9^-$-minus-PQ-9 difference FT-IR spectrum, with no ethanol contribution, obtained as described above for decyl PQ. (C, dotted line) shows the corresponding negative control, obtained before the addition of reductant. The concentration of PQ-9 in (C) was 5 mM. The tick marks on the *y* axis correspond to 1×10^{-2} absorbance units. See Materials and Methods for additional experimental details.

assigned to the semiquinone anion radical of decyl PQ. The 1587 cm^{-1} region of the spectrum contained a relatively intense, overlapping ethanol band (Figure 3A, dotted line), so this part of the spectrum was not assigned.

The difference spectrum associated with the one electron reduction of PQ-9 was also obtained (Figure 3C, solid line). Again, data obtained before addition of reductant gave a flat baseline (Figure 3C, dashed line). The spectrum associated with the reduction of PQ-9 resembled, but was not identical to, the spectrum obtained from decyl PQ. The pattern of negative lines was indistinguishable, but additional spectral complexity and frequency shifts were observed in positive features, with the semiquinone anion radical of PQ-9 giving rise to positive lines at 1471, 1452, 1409, 1373, 1333, and 1308 cm^{-1} (Figure 3C, solid line).

In Vivo Studies of Q_A and Q_A^-. In parts A and B of Figure 4, we present the mass spectra of PQ-9 samples, which were isolated from a methionine-tolerant strain of *Synechocystis sp.* PCC 6803. Cyanobacterial cultures were supplied L-methionine

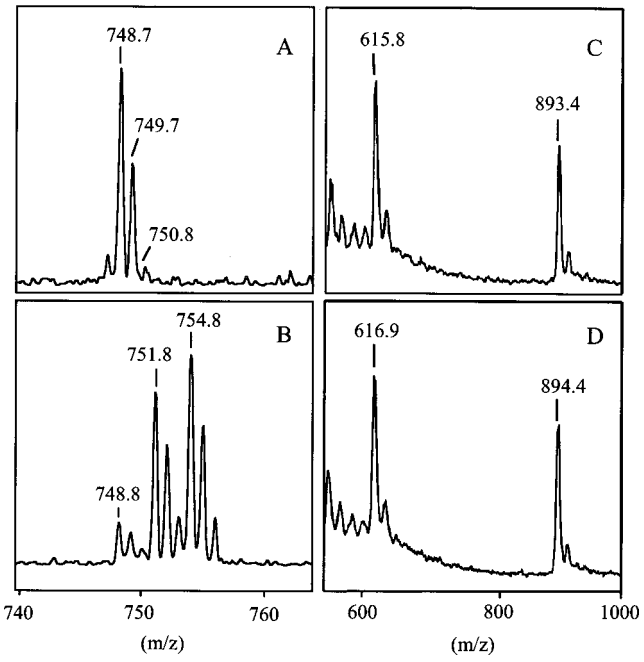

Figure 4. Electrospray mass spectrum of PQ-9, extracted from cyanobacteria grown either on 200 μM L-methionine (A) or L-$^2H_3$-methionine (B). Plasma desorption mass spectrum of chl *a* extracted from cyanobacteria grown either on 200 μM L-methionine (C) or L-$^2H_3$-methionine (D).

(Figure 4A). As expected under these conditions,[13,34] the most abundant molecular ion of PQ-9 had a mass of 749 (Figure 4A). The observed shift of the mass spectrum to higher molecular mass, when PQ-9 was extracted from cultures grown on L-$^2H_3$-methionine (Figure 4B), was consistent with the expected incorporation of deuterium into the methyl groups of PQ-9.[13] Because methionine is a methyl group donor in biosynthetic reactions, three deuterium atoms are expected to be incorporated per methyl group. Analysis of these data reveals that 39% of PQ-9 was $^2H_3$ labeled at one methyl group and that 48% was $^2H_6$ labeled at both methyl groups. Overall, 87% of the compound was isotopically labeled and only 13% was unlabeled. These values are in good agreement ($\pm$1%) with data previously obtained through the use of an *Anabaena variabilis* methionine auxotroph.[13] Plasma desorption mass spectral analysis also provided evidence for ^2H incorporation into the methyl groups of PQ-9 in these cultures (data not shown).

Chl was also isolated from unlabeled (Figure 4C) cultures, and plasma desorption mass spectrometry was used to measure the molecular mass.[34] The chl molecular ion has a mass of 893.4 $\pm$ 0.1; the fragment at 615.8 $\pm$ 0.1 (Figure 4C) arises from loss of the esterifying phytol alcohol from the intact chl a molecule (see ref 34 and references therein). When cells were grown on $^2H_3$ methionine, a shift was observed to 894.4 $\pm$ 0.6 and 616.9 $\pm$ 0.9 (Figure 4D). Electrospray mass spectroscopy suggests that 68% of the chl a sample is $^2H_3$ labeled (data not shown), accounting for the observed 1 amu increase in the plasma desorption data (Figure 4C and D). The only methyl group of chl a potentially derived from methionine is the 13^3 methoxy group.[76] We conclude that while the chl macrocyle is unlabeled, the majority of the chl sample may be $^2H_3$ labeled at the 13^4 position. When cells were grown on $^2H_3$ methionine, there was no detectable deuterium incorporation into the phytol tail, as judged by comparison of molecular and fragment ions, which both show a 1 amu increase (compare parts C and D of Figure 4).

In Figure 5, we present a difference (light-minus-dark) FT-IR spectrum obtained from cyanobacterial PSII samples. The spectra were recorded, and illumination was performed at 80 K. The light-induced difference spectrum reflects contributions from the vibrational modes of cofactors and amino acid residues that undergo structural changes upon light-induced electron transfer. The cyanobacterial PSII preparation employed has been shown to contain low-potential cytochrome b-559.[60] Therefore, this species is already oxidized in this PSII preparation and is not available to act as an electron donor.[61,62] Illumination at 80 K is expected to result primarily in the oxidation of chl[31,32,61,62] and the reduction of Q_A (but see below for a discussion of the possibility that carotenoid may be oxidized in some PSII centers). The difference FT-IR spectrum resembles ($\pm$1 cm^{-1}) spectra previously reported for chl$^+Q_A^-$-minus-chlQ_A in spinach PSII.[31,32] Under these conditions, the photoaccumulation of Q_A^- has been shown to be optimal.[31,32] Therefore, a subset of the vibrational bands observed in Figure 5 is expected to be derived from the Q_A^--minus-Q_A vibrational spectrum.

Particularly important is the fact that these conditions minimize contributions to the difference infrared spectrum from redox tyrosines in PSII.[31−33] In our previous work, we have presented EPR control experiments showing that tyrosine D and Z do not contribute to the difference FT-IR spectrum, obtained under this set of conditions.[31−33] These neutral tyrosyl radicals contribute to the spectrum at 1478/1477 cm^{-1},[19,63−67] so a contribution from these species would complicate the region where Q_A^- contributions would be expected (see Figure 3C).

To identify quinone and semiquinone anion contributions, spectra were obtained from PSII, isolated from cyanobacterial cultures supplied with methionine (Figure 5A) or with $^2H_3$-methionine (Figure 5B). The data shown in parts A and B of Figure 5 were normalized on the basis of the total amount of protein present in the FT-IR sample and were also corrected for any differences in path length.[31−33] An isotope-edited, ^1H-minus-^2H, double difference spectrum (Figure 5C, solid line) was then constructed by direct one-to-one subtraction of these spectra. ^2H induced shifts in vibrational lines were observed, resulting in the appearance of a spectral feature with the opposite sign. These lines were not observed in a control ^1H-minus-^1H double difference spectrum (Figure 5C, dashed line), indicating that nonisotope sensitive lines cancel.

As shown in Figure 5C, solid line, ^2H-sensitive vibrational modes were observed in the 1480−1460 and 1650 cm^{-1} spectral regions. Comparison to PQ$^-$-minus-PQ data obtained in vitro (Figure 3C, solid line) suggests that these lines are assignable to CO and ring CC stretching vibrations of plastoquinone and the plastosemiquinone anion radical in PSII.

In the 1480−1460 cm^{-1} region (Figure 5C, solid line), positive lines at 1482 and 1469 cm^{-1} are assigned to Q_A^-. The positive line at 1482 cm^{-1} exhibited a 5 cm^{-1} downshift to 1477 cm^{-1} upon methyl deuteration (compare parts A and B of Figure 5, and also part C, solid line). Although a positive line at 1469 cm^{-1} was also observed in the isotope-edited spectrum, the location of the downshifted line corresponding to this feature was not obvious due to the complexity of this spectral region. This complexity may be caused by the pattern of isotopic labeling, in which 39% of PQ-9 was $^2H_3$ labeled and 48% was $^2H_6$ labeled. Overall, significant intensity differences in the 1480−1420 cm^{-1} region may be caused by the downshift of C−H bending modes out of this spectral range in deuterated samples (see discussion below). The 1482 cm^{-1} line may be analogous to the 1471 cm^{-1} line observed in data obtained from PQ-9$^-$ in vitro (Figure 3C, solid line). This assignment suggests

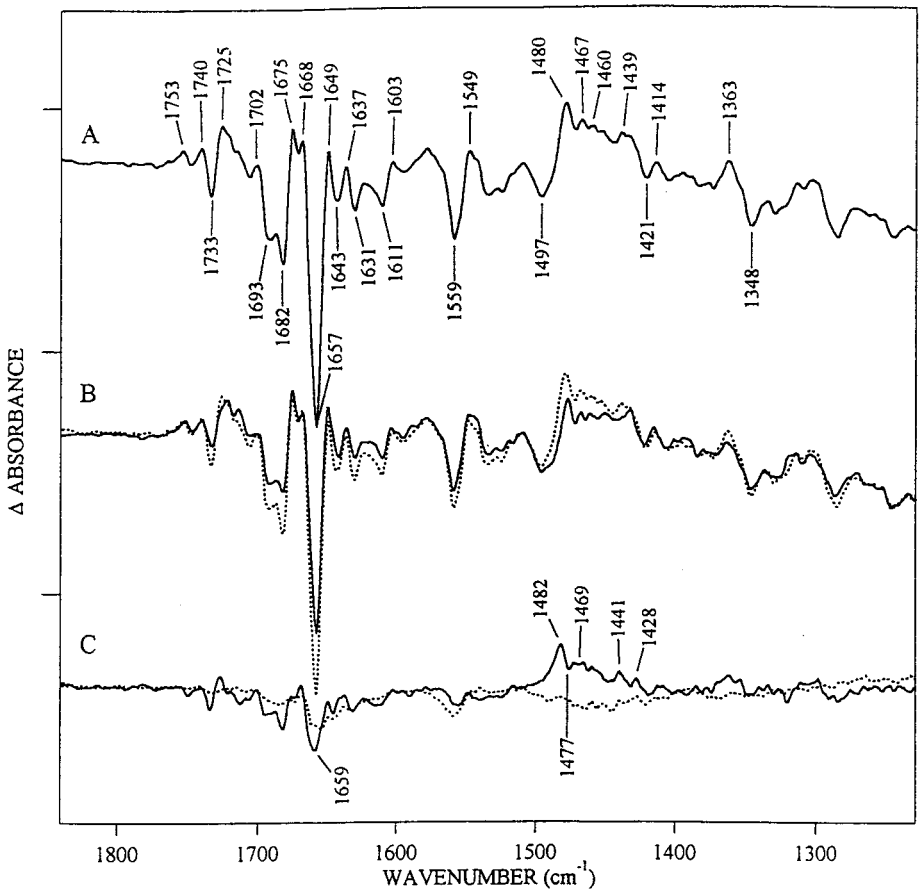

Figure 5. Light-minus-dark difference FT-IR spectra of PSII preparations isolated from cyanobacteria grown either on 200 μM L-methionine (A) or L-$^2H_3$-methionine (B, solid line). Spectrum (A) is repeated in (B) as the dotted line to facilitate comparison. Spectra shown in (A) and (B, solid line) are the average of 12 and 10 light-minus-dark difference spectra, respectively. The spectrum shown in (C, solid line) is a ^{1}H-minus-^{2}H double-difference spectra calculated from the direct 1:1 subtraction of (A)-minus-(B). Data shown in (C, dashed line) are a control ^{1}H-minus-^{1}H double difference spectrum. Individual difference spectra were corrected for path length and protein concentration before data manipulation. The tick marks on the *y* axis correspond to 2×10^{-3} absorbance units.

a significant, 11 cm^{-1} upshift when PQ-9$^-$ vibrational modes in PSII are compared to data obtained in ethanolic solutions, which may be caused by a change in the strength of hydrogen bonding.

Comparison of PSII data (Figure 5C, solid line) with in vitro data (Figure 3C, solid line) suggests that Q_A vibrational modes should contribute to the PSII spectrum in the 1650 cm^{-1} spectral region. The ^{1}H-minus-^{2}H isotope edited spectrum exhibited deuterium-sensitive vibrational modes in this spectral region (Figure 5C), which will be discussed in more detail below.

Because methionine is $^2H_3$-labeled, in addition to incorporation of deuterium into PQ-9 there may also be minor incorporation of deuterium into PSII protein subunits. Minor ^{2}H incorporation into PSII subunits would result in overlapping spectral contributions to the isotope edited spectrum in the 1800−1200 cm^{-1} region. The 13^3 methoxy group of chl is also deuterated, so chl$^+$-minus-chl may contribute to the 1800−1200 cm^{-1} region of the isotope-edited spectrum. In vitro difference infrared studies, in which a chl cation radical was generated, have shown that the only intense vibrational mode of this group is the carbonyl stretch, which, as expected, absorbs at 1751 (chl$^+$) and 1738 cm^{-1} (chl).[77] Other ester vibrational modes expected are the CO vibration, below 1300 cm^{-1}, and CH bending modes, which shift below 1200 cm^{-1} upon deuteration (see results below).[77] Thus, chl$^+$-minus-chl contributions should be distinguishable from Q_A^--minus-Q_A contributions.

Normal Modes of Hydrogen Bonded Plastoquinone. The computational model of plastoquinone-1 with two water molecules (PQ+2H_2O) had 87 vibrational normal modes. Table 1 shows that the four highest frequency modes were O−H stretches in the water molecules surrounding the quinone. The next 12 highest frequency modes were C−H stretches in the quinone. Bending motions in the water molecules surrounding the quinone appeared at frequencies of 1671 and 1659 cm^{-1}. The modes at 1664 and 1632 cm^{-1} had motions that involved primarily ring C═C/CO symmetric stretching. The lower frequency mode, at 1632 cm^{-1}, was predominantly CO symmetric stretching, whereas the higher frequency, 1664 cm^{-1}, mode was predominantly C═C stretching. Next, a mode with mainly isoprenoid C═C stretching character appeared at 1657 cm^{-1}. Substitution of the chain-terminal hydrogens by tritium shifted this mode to 1559 cm^{-1} and demonstrated that its appearance at 1657 cm^{-1} was the result of replacing the chain-terminal methyl groups with much lighter hydrogens. A CO antisymmetric stretch was calculated at 1649 cm^{-1}, and an antisymmetric ring C═C stretch was calculated at 1604 cm^{-1} (Table 1).

Of the 26 frequencies between 1473 and 940 cm^{-1}, 19 were assigned to primarily C−H bending motions, five modes had significant amounts of both C−H bending and C−C stretching motions, and two modes were assigned to C−C stretches. The mode appearing at 1438 cm^{-1} involved primarily C−H bending of the methylene hydrogen atoms of the isoprenyl chain. The mode calculated at 1417 cm^{-1} involved chain C−H bending, but shifted out of this frequency range when tritium was substituted for the chain-terminal hydrogens. Thus, the mode calculated at 1417 cm^{-1} appeared at this frequency only because

TABLE 1: Comparison of Calculated Scaled Harmonic Vibrational Frequencies (cm^{-1}) for Plastoquinone-1 and Its Radical Anion, Each Interacting with Two Water Molecules[a]

description	$PQ+2H_2O$	$PQ^{\bullet-}+2H_2O$	description	$PQ+2H_2O$	$PQ^{\bullet-}+2H_2O$
O−H stretch (water)	3673	3639	C−H bend (ring)	994	952
O−H stretch (water)	3656	3637	C−H bend (methyl)	987	985
O−H stretch (water)	3557	3323	C−C stretch	957	967
O−H stretch (water)	3499	3237	C−H bend (chain)	950	903
C−H stretch (chain)	3111	3090	C−H bend (chain)	940	937
C−H stretch (ring)	3062	3052	ring/chain distortion	924	915
C−H stretch (methyl)	3051	3045	ring distortion	832	860
C−H stretch (methyl)	3050	3026	ring torsion	800	776
C−H stretch (chain)	3049	3056	ring torsion	752	746
C−H stretch (chain)	3032	3017	ring torsion	702	694
C−H stretch (chain)	2986	2957	chain torsion/ring breathing	666	667
C−H stretch (methyl)	2980	2934	ring rock	650	653
C−H stretch (methyl)	2973	2931	water bend	635	852
C−H stretch (methyl)	2932	2897	ring breathing	561	569
C−H stretch (chain)	2931	2907	ring torsion	526	538
C−H stretch (methyl)	2929	2899	water-ring breathing	483	493
water bend	1671	1704	water bend	468	470
ring C═C/C═O symmetric stretch	1664	1602	water bend	454	470
water bend	1659	1697	ring bend	431	424
chain C═C stretch	1657	1656	ring bend	426	434/437
C═O antisymmetric stretch	1649	1482	ring bend	376	381/373
ring C═C/C═O symmetric stretch	1632	1467	ring bend	346	353
ring C═C antisymmetric stretch	1604	1498	water bend	317	437
C−H bend (methyl)	1473	1487	methyl-ring bend	308	328
C−H bend (methyl)	1458	1468	torsion	285	302
C−H bend (methyl)	1451	1464	torsion	266	286
C−H bend (methyl)	1449	1451	water/chain torsion	245	220
C−H bend (methylene)	1438	1432	water bend	225	199
C−H bend (chain)	1417	1413	water bend	214	199
C−H bend (methyl)	1381	1378	water/chain torsion	191	249
C−H bend (methyl)	1374	1356	water quinone stretch	156	179
C−C stretch, C−H bend (ring)	1343	1400	water quinone stretch	146	186
C−H bend (chain)	1307	1257	chain torsion/water	138	151
C−H bend (methyl), C−C stretch (ring)	1290	1304	methyl wagging	112	137
C−H bend (chain)	1285	1287	methyl twist	104	135
C−C stretch, C−H bend (chain, ring)	1247	1202	chain/methyl/water	97	61
C−H bend (chain, ring)	1201	1208	chain/methyl/water torsion	89	88/74
C−C stretch	1174	1181	chain/methyl torsion	80	113
C−H bend(methyl), C−C stretch	1095	1100	methyl twist	68	107
C−H bend (methylene)	1084	1080	chain/methyl torsion	53	61
C−H bend, C−C stretch	1075	1084	chain/methyl torsion	48	74/53
C−H bend (chain)	1042	1021	chain torsion	33	74/37
C−H bend (methyl)	1034	1037	chain torsion	19	16
C−H bend (methyl)	1001	1008			

[a] Calculations were done using the B3LYP Hartree−Fock/Density Functional method and a 6-31G(d) basis set. Modes above 1000 cm^{-1} were scaled by 0.9614; modes below 1000 cm^{-1} were scaled by 1.0013.

of necessary structural model simplification. Other C−H bending modes in the similar frequency range involved primarily *methyl* C−H bending motions. Below 1000 cm^{-1}, calculated modes included a variety of torsions involving complicated motions of the atoms.

Normal Modes of Deuterated, Hydrogen Bonded Plastoquinone. Complete deuteration of the methyl groups (PQ-d_6+$2H_2O$) shifts the methyl C−H bending modes below 1200 cm^{-1}. As expected, the water bending modes were unshifted and appeared at 1671 and 1659 cm^{-1}. The ring C═C/CO symmetric stretches at 1664 and 1632 cm^{-1} shifted to 1663 and 1631 cm^{-1}, respectively, in PQ-d_6+$2H_2O$. The CO antisymmetric stretch shifted from 1649 to 1648 cm^{-1}, and the ring C═C antisymmetric stretch downshifted from 1604 to 1598 cm^{-1}. Below 1598 cm^{-1}, the next three modes of PQ-d_6+$2H_2O$ were calculated at 1439 cm^{-1} (C−H bend-chain), 1417 cm^{-1} (C−H bend-chain), and 1345 cm^{-1} (C−C stretch-ring). These modes appeared at 1438, 1417, and 1343 cm^{-1}, respectively, in PQ+$2H_2O$. Thus, except for the methyl C−H bends, most modes of PQ+$2H_2O$ downshifted 1−6 cm^{-1} upon complete methyl deuteration.

Normal Modes of the Hydrogen Bonded Plastosemiquinone Anion Radical. Table 1 also presents calculated vibrational frequencies for the model of plastosemiquinone anion radical with two water molecules ($PQ^{\bullet-}+2H_2O$). The four highest frequency modes were O−H stretches, and the next 12 were C−H stretches. At 1704 and 1697 cm^{-1}, water bending modes appeared. The calculated shift of O−H stretching modes to lower frequencies and water bending modes to higher frequencies, upon reduction of PQ+$2H_2O$, is consistent with stronger hydrogen bonding between water and the charged $PQ^{\bullet-}$ ion. The C═C stretch from the isoprenoid chain occurred at 1656 cm^{-1}, and once again this mode shifted far from this frequency range when masses more similar to the real methyl masses were used in the calculation. A symmetric CC ring stretch appeared at 1602 cm^{-1}, and a symmetric CO stretch was calculated at 1467 cm^{-1}. The antisymmetric CC ring stretch was calculated at 1498 cm^{-1}, and the antisymmetric CO stretch was calculated at 1482 cm^{-1}. Table 1 shows that the next highest frequency vibrational modes involved C−H bending (19 modes), C−C stretching (two modes), and a combination of C−C stretching and C−H bending (five modes). The C−H bending

mode calculated at 1413 cm^{-1} appeared at this frequency due to replacement of chain-terminal methyls with hydrogen in the PQ-1 model. The modes below 1000 cm^{-1} were similar to those of PQ+2H_2O and were primarily torsions involving complicated atomic motions.

Normal Modes of the Deuterated Hydrogen Bonded Plastosemiquinone Anion Radical. Upon deuteration of both methyl groups, the plastosemiquinone anion ($PQ^{\bullet -}$-d_6+2H_2O) showed isotopic frequency shifts somewhat larger than those described for PQ+2H_2O (see Supporting Information). The highest frequency symmetric CC ring stretch of the anion radical shifted from 1602 to 1600 cm^{-1}, and the symmetric CO stretch shifted from 1467 to 1461 cm^{-1}. The antisymmetric CO stretch shifted from 1482 to 1477 cm^{-1}, and the antisymmetric CC stretch shifted from 1498 to 1490 cm^{-1}. The next three modes in the deuterated model were at 1432 cm^{-1} (C−H bending-chain), 1413 cm^{-1} (C−H bending-chain), and 1404 cm^{-1} (C−H bending-chain)/CC stretching) and were similar to the modes at 1432, 1413, and 1400 cm^{-1}, respectively, in the undeuterated $PQ^{\bullet -}$+ 2H_2O. All of the modes involving methyl C−H bending downshifted below 1200 cm^{-1} upon methyl deuteration.

Discussion

The difference spectrum associated with the reduction of PQ-9 has been obtained and assigned in this investigation. Analysis of this spectrum is important in understanding the mechanism of electron transfer to the acceptor side of PSII. To our knowledge, this is the first report of the PQ-9 anion radical spectrum in vitro. Previously, the vibrational spectra of UQ and its anion radical were used to predict this vibrational spectrum. However, based on the chemical structure, the vibrational spectra of PQ and its anion radical are expected to differ from those of UQ. For example, differences between the vibrational spectra of PQ and UQ were observed in the FT-IR data of diradicals generated by UV irradiation.[25]

While the assignment of isotope-shifted lines to Q_A and Q_A^- relies on a comparison to the PQ-9 spectrum obtained in vitro, the vibrational spectrum of PQ-9 in the Q_A site is not necessarily the same as that of PQ-9 in solution. Indeed, our experiments suggest that approximately 6−11 cm^{-1} frequency shifts occur in the protein environment, perhaps from hydrogen bonding alterations. To identify the spectral features of Q_A and Q_A^-, we have developed a method to label PQ-9 in a cyanobacterium, *Synechocystis sp.* PCC 6803. The advantages of this organism are that PSII can be purified for study and that site-directed mutants can be created in the environment of Q_A.[15] This method of labeling PQ-9 results in the incorporation of deuterium into the methyl groups of the molecule.[13] Approximately 87% of PQ-9 is isotopically labeled by this method. This method will identify vibrational modes of Q_A^- and Q_A that show sensitivity to methyl deuteration. In calculations with both methyl groups completely deuterated, methyl C−H bending vibrations shifted to frequencies below 1200 cm^{-1}. Nine additional vibrational modes in the 1800−1200 cm^{-1} region showed sensitivity to methyl labeling (omitting the water-based and chain C═C modes).

A previous assignment of the Q_A^- CO stretching vibration to 1478 cm^{-1} has been made.[68] However, this assignment was not based on isotope identification, and the spectra obtained may have also exhibited contributions from tyrosyl radicals,[19,63−67] which overlap this spectral region and complicate its interpretation. Further complicating this spectral region is a ^{15}N-sensitive vibrational mode of chl^+.[69] Based on the current literature,[77,78] a ^{15}N-sensitive chl macrocycle vibration at 1478 cm^{-1} would not be expected to be sensitive to deuteration at the 13^3 methoxy position and thus would not contribute to the $^2H_3$-methionine isotope-edited spectrum.[78] However, this possibility is under further investigation.

TABLE 2: Mode Assignments, Experimentally Measured Vibrational Frequencies (cm^{-1}), and Calculated Harmonic Vibrational Frequencies (cm^{-1})

neutral quinone	decyl-PQ/PQ-9	Q_A	B3LYP
CO antisymmetric stretch	1653/1652	1659[a]	1649
ring C═C/CO symmetric stretch	1633	1631[a]	1632
ring C═C antisymmetric stretch	1617/1618	1611[a]	1604
semiquinone anion radical	**decyl-PQ^-/PQ-9^-**	**Q_A^-**	**B3LYP**
ring CC antisymmetric stretch	1474/1471	1482[a]	1498
CO antisymmetric stretch	1454/1452	1469[a]	1482
ring C−H bend/C−C stretch	1418/1409	*b*	1400
CO symmetric stretch		*b*	1467
methyl C−H bend		*b*	1468

[a] Tentative assignment. [b] Vibrational modes observed in this spectral region, but not assigned.

Below, we give a preliminary assignment of the vibrational spectra obtained in vivo and in vitro. This assignment is based on the normal mode calculations previously presented for PQ-9 and its anion radical[29] and the calculations shown here. Table 2 summarizes mode assignments obtained by comparing experimentally observed bands with mode frequencies, intensities, and isotopic frequency shifts calculated in this work.

Preliminary Assignment of the in Vitro Spectrum of Decyl-PQ and PQ-9. The vibrational spectrum of PQ-9 has been reported previously,[25,70] and the spectrum has been shown to be influenced by the formation of dimeric and oligomeric complexes.[70] Therefore, it was necessary to obtain all vibrational spectra in the same solvent and then to subtract solvent contributions from the spectrum. The spectra obtained in this paper are in agreement with PQ-9 frequencies reported previously.[25,70]

With the aid of normal mode calculations for PQ+2H_2O, a portion of the vibrational spectrum of decyl PQ and PQ-9 can be assigned. First, the experimental vibrational band observed at 1653/1652 cm^{-1} in decyl PQ/PQ-9 can potentially be assigned to the calculated frequencies at 1664 (ring C═C/CO symmetric stretch) or 1649 (CO antisymmetric stretch) cm^{-1} (Table 1). The C═C chain stretching mode calculated at 1657 cm^{-1} was eliminated from this consideration, because the experimentally measured band appears in the spectrum of decyl PQ, which has no chain C═C, and because the calculated C═C chain stretching mode should appear in a completely different frequency range for the real plastoquinone, based on tests described earlier. Of the two remaining possibilities, we prefer to assign the observed 1653/1652 cm^{-1} band to the CO antisymmetric stretching mode, calculated at 1649 cm^{-1} (Table 2), because the calculated IR intensity of the CO mode is nearly 2 orders of magnitude higher than the intensity of the mode calculated at 1664 cm^{-1}.

The experimental band at 1633 cm^{-1} in decyl PQ/PQ-9 is assigned to a ring C═C/CO symmetric stretch calculated to appear at 1632 cm^{-1}, and the 1618/1617 cm^{-1} band is assigned to an antisymmetric ring C═C stretching mode, calculated at 1604 cm^{-1} (Tables 1 and 2).

Assignment of the in Vitro Spectrum of the Semiquinone Anion Radical. The primary effects of reducing PQ to a semiquinone anion radical are expected to be on the frequencies of the CO and ring CC stretching modes. These effects are due to a change in bond length caused by electron addition to the aromatic ring.[29,71,72] In a previous computational study of non-

hydrogen bonded plastoquinone, the CC vibrational modes of the anion radical were calculated at higher frequencies when compared to the CO vibrational modes.[29] This effect is also observed in our calculations (Table 1) on the hydrogen bonded molecule.

The decyl PQ^- and PQ-9^- anion radical vibrational spectrum can be assigned based on the calculated vibrational frequencies shown in Table 1. The spectral feature at 1474/1471 cm^{-1} (decyl PQ^-/PQ-9^-) is assigned to an antisymmetric CC ring stretching mode. This CC ring stretching mode is present in the calculations at 1498 cm^{-1}. The band at 1454/1452 cm^{-1} (decyl PQ^-/PQ-9^-) is assignable to the CO antisymmetric stretch and is calculated to appear at 1482 cm^{-1} (Table 2). These two modes, calculated at 1498 and 1482 cm^{-1}, have approximately equal calculated IR intensities, and their calculated intensities are nearly an order of magnitude larger than those of other bands calculated to appear in the same spectral region. The experimental vibrational mode at 1418/1409 cm^{-1} can be assigned to one of many C−H bending modes that appear in that region or to a mixed C−C stretch/C−H bend seen in the calculations at 1400 cm^{-1} with a moderately high calculated IR intensity (Table 2). The vibrational modes between 1373 and 1308 cm^{-1} could arise from methyl, decyl, and/or isoprenoid C−H bending motions.

Preliminary Assignment of the in Vivo Q_A Spectrum. Unique vibrational modes of unlabeled Q_A make negative contributions to the ^{1}H-minus-^{2}H, isotope edited, double difference spectrum (Figure 5C, solid line). On the basis of model compound studies presented here, these contributions are expected in the 1660−1610 cm^{-1} region of the spectrum. Overlapping vibrational bands arising from the amide I vibration of the peptide backbone are also expected in this spectral region.[31]

In the 1650 cm^{-1} region of the isotope-edited spectrum (Figure 5C, solid line), a negative line is observed at 1659 cm^{-1}. Comparison of these data with the spectrum associated with the reduction of PQ in vitro (Figure 3) and with a control ^{1}H-minus-^{1}H double difference spectrum (Figure 5C, dotted line) suggests that this line may be assignable to a CO antisymmetric stretching mode of Q_A (Table 2). This vibrational frequency is calculated at 1649 cm^{-1} (Table 1). However, this is a tentative assignment, due to the possible minor incorporation of deuterium into PSII subunits, the low intensity of spectral features in this region of the double difference spectrum (Figure 5C, solid line), and the small magnitude of the expected isotope shift (1 cm^{-1}).

Lines observed in the difference spectrum, $chl^+Q_A^-$ -minus-$chlQ_A$ (Figure 5A), at 1631 and 1611 cm^{-1} are candidates to be the ring C═C/CO symmetric and ring C═C antisymmetric stretching modes of Q_A, respectively. The amplitudes of these lines were observed to be relatively temperature independent, when data were acquired and illumination was performed at 200, 130, and 80 K.[31,32] Because this experimental protocol is expected to change the identity of electron donor(s), while leaving the Q_A contribution to the spectrum unchanged, this previous result tends to support our assignment of these lines to Q_A. However, any contributions to the ^{1}H-minus-^{2}H spectrum (Figure 5C, solid line) at 1631 and 1611 cm^{-1} are below our detection limit, so this assignment also remains tentative (Table 2).

Preliminary Assignment of the in Vivo Q_A^- Spectrum. Unique vibrational modes of unlabeled Q_A^- make positive contributions to the ^{1}H-minus-^{2}H, isotope edited, double difference spectrum (Figure 5C, solid line). On the basis of model compound studies, positive lines are expected with frequencies between 1480 and 1300 cm^{-1}. The isotope-edited spectrum (Figure 5C, solid line) exhibits a positive 1482 cm^{-1} line, which we assign to an antisymmetric CC ring stretching vibration of Q_A^- (Table 2). This vibrational frequency is calculated at 1498 cm^{-1} (Table 1). The downshifted spectral feature corresponding to this vibrational mode after methyl deuteration is apparently located at 1477 cm^{-1}. This observed isotopic shift of −5 cm^{-1} corresponds well to the calculated maximum shift of −8 cm^{-1}.

A positive experimental band is also observed at 1469 cm^{-1}. This band can be assigned to the CO antisymmetric stretch of Q_A^-, which is calculated to be at 1482 cm^{-1} (Table 1). Because of the complexity of this spectral region, the magnitude of the isotope-induced downshift is not obvious from analysis of the double difference spectrum (Figure 5C, solid line).

The appearance of lines at 1480 and 1469 cm^{-1} was observed to be temperature dependent when data were acquired and illumination was performed at 200, 130, and 80 K.[31,32] Although this experimental protocol is expected to leave the Q_A^- contribution to the spectrum unchanged, cancellation of intensity in the difference spectra can explain this result. We have observed that contributions to the difference FT-IR spectrum from amino acid residues ligated to or in proximity to the manganese cluster are relatively intense, compared to Q_A and Q_A^- contributions.[19,31,32]

Other vibrational bands, observed between 1441 and 1428 cm^{-1}, can potentially be assigned to the following modes in Table 1: the CO symmetric stretch (calculated at 1467 cm^{-1}); methyl C−H bending modes (calculated with a similar IR intensity at 1468 cm^{-1}); C−C stretching/ring C−H bending modes (calculated at 1400 cm^{-1}); and, possibly, C−H bending modes of the isoprenoid chain's methylene group (Table 2). The overall change in intensity in this region upon methyl deuteration may be due to the downshift of methyl C−H bending modes to the spectral region below 1200 cm^{-1}.

Summary. We conclude that the difference FT-IR spectrum associated with reduction of Q_A in PSII has components at 1659 (neg. Q_A), 1482 (pos. Q_A^-), and 1470/1467 (pos. Q_A^-) cm^{-1}. The corresponding lines in vitro are observed at 1653, 1471, and 1452 cm^{-1}. Calculated frequencies, IR intensities, and/or isotopic frequency shifts suggest these lines can be assigned to the CO antisymmetric stretching mode of PQ (calculated at 1649 cm^{-1}), the CC ring antisymmetric stretching mode of PQ^- (calculated at 1498 cm^{-1}), and the CO antisymmetric stretch of PQ^- (calculated at 1482 cm^{-1}), respectively. These three modes have the highest calculated IR intensities of the quinone-based modes in this spectral region. This set of assignments assumes that deuteration of the chl 13^3 methoxy group does not induce a significant chl^+-minus-chl contribution to these regions of the isotope-edited spectrum.

The measured intensity of the 1482 cm^{-1} spectral features arising from Q_A^- is on the order of 4×10^{-4} absorbance units. This value is based on an amide II band of 0.5 absorbance units; the molecular mass of the cyanobacterial PSII preparation is approximately 250 000 Da. This value is similar to the intensity of the corresponding Q_A^- band in the bacterial reaction center (protein molecular weight of approximately 125 000), which has been reported as 5×10^{-4} absorbance units.[73]

Recently, evidence supporting carotenoid oxidation in a manganese-depleted plant PSII preparation, treated with a high concentration (0.5%) of lauryl maltoside, has been reported.[74] The EPR signal, attributed to the PSII carotenoid cation radical (car^+), was similar to the EPR signal of chl^+.[74] Carotenoid was photo-oxidized in the minority of centers at 77 K; the amount

of car$^+$ produced was 19% of the maximum, which was generated by a 20 K illumination. On the other hand, the amount of chl$^+$ produced at 77K was 72% of the maximum. If carotenoid is photooxidized in our PSII preparation at 80 K, the conclusions of our work remain unaltered. Mass spectral data presented here provides no evidence for significant labeling of the phytol tail of chl. Because phytol and carotenoids share a common biosynthetic precursor,[75] this result implies that carotenoids are not significantly labeled from deuterated methionine.

In future work, we will use vibrational spectroscopy to investigate electron transfer to Q_A and Q_B in PSII.

Acknowledgment. This work was supported by a grant from the National Science Foundation, MCB 98-08934 (B.A.B), by an NIH predoctoral fellowship to I. A., and by grants to R. A. W. from the U.S. Department of Energy through Contract DE-FG03-97ER14806, the Oklahoma Center for the Advancement of Science and Technology (OCAST Award H97-091), and the National Science Foundation/National Resource Allocations Committee (Award MCA96N019 at the NSF/National Computational Science Alliance facilities at the University of Illinois Urbana-Champaign). We are grateful to the National Science Foundation and Silicon Graphics Corporation for funding supercomputers located at the University of Oklahoma.We are also grateful to Prof. David Kramer (Washington State University) for helpful discussions and to Prof. Alan Hooper and his laboratory (University of Minnesota) for the use of the diode array spectrophotometer. We thank Kelly Halverson for assistance in data acquisition. Mass spectral analysis was performed at the University of Minnesota Mass Spectrometry Consortium for the Life Sciences.

Supporting Information Available: Eight tables containing Cartesian coordinates for optimized structures of PQ+2H_2O and PQ$^{\bullet-}$+2H_2O, vibrational mode assignments and frequencies for PQ, PQ+2H_2O, PQ$^{\bullet}$, and PQ$^{\bullet-}$+2H_2O, and vibrational projection analysis relating modes for the pairs of structures PQ/PQ+2H_2O, PQ+2H_2O/PQ$^{\bullet-}$+2H_2O, PQ+2H_2O/PQ-d_6+2H_2O, and PQ$^{\bullet-}$+2H_2O/PQ$^{\bullet-}$-d_6+2H_2O. This material is available free of charge via the Internet at http://pubs.acs.org.

References and Notes

(1) Britt, R. D. In *Oxygenic Photosynthesis: The Light Reactions*; Ort, D. R., Yocum, C. F., Eds.; Kluwer Academic Publisher: Dordrecht, 1996; Vol. 4, pp 137−164.
(2) Deisenhofer, J.; Epp, O.; Miki, K.; Huber, R.; Michel, H. *Nature* **1985**, *318*, 618−624.
(3) Ermler, U.; Michel, H.; Schiffer, M. *J Bioenerg. Biomembr.* **1994**, *26*, 5−15.
(4) Debus, R. J.; Barry, B. A.; Sithole, I.; Babcock, G. T.; McIntosh, L. *Biochemistry* **1988**, *27*, 9071−9074.
(5) Gerken, S.; Brettel, K.; Schlodder, E.; Witt, H. T. *FEBS Lett.* **1988**, *237*, 69−75.
(6) Metz, J. G.; Nixon, P. J.; Rögner, M.; Brudvig, G. W.; Diner, B. A. *Biochemistry* **1989**, *28*, 6960−6969.
(7) Noren, G. H.; Barry, B. A. *Biochemistry* **1992**, *31*, 3335−3342.
(8) Boerner, R. J.; Barry, B. A. *J. Biol. Chem.* **1993**, *268*, 17151−17154.
(9) Razeghifard, M. R.; Klughammer, C.; Pace, R. J. *Biochemistry* **1997**, *36*, 86−92.
(10) Joliot, P.; Barbieri, G.; Chabaud, R. *Photochem. Photobiol.* **1969**, *10*, 309−329.
(11) Buser, C. A.; Thompson, L. K.; Diner, B. A.; Brudvig, G. W. *Biochemistry* **1990**, *29*, 8977−8985.
(12) Buser, C. A.; Diner, B. A.; Brudvig, G. W. *Biochemistry* **1992**, *31*, 11449−11459.
(13) Barry, B. A.; Babcock, G. T. *Proc. Natl. Acad. Sci. U.S.A.* **1987**, *84*, 7099−7103.
(14) Boerner, R. J.; Barry, B. A. *J. Biol. Chem.* **1994**, *269*, 134−137.
(15) Barry, B. A. *Photochem. Photobiol.* **1993**, *57*, 179−188.
(16) Svensson, B.; Vass, I.; Cedergen, E.; Styring, S. *EMBO J.* **1990**, *9*, 2051−2059.
(17) Ruffle, S. V.; Donnelly, D.; Blundell, T. L.; Nugent, J. H. A. *Photosynth. Res.* **1992**, *34*, 287−300.
(18) Braiman, M. S.; Rothschild, K. J. *Annu. Rev. Biophys. Biophys. Chem.* **1988**, *17*, 541−570.
(19) Kim, S.; Ayala, I.; Steenhuis, J. J.; Gonzalez, E. T.; Razeghifard, M. R.; Barry, B. A. *Biochim. Biophys. Acta* **1998**, *1366*, 330−354.
(20) Buchanan, S.; Michel, H.; Gerwert, K. *Biochemistry* **1992**, *31*, 1314−1322.
(21) Zhao, X.; Ogura, T.; Okamura, M.; Kitagawa, T. *J. Am. Chem. Soc.* **1997**, *119*, 5263−5264.
(22) Breton, J.; Burie, J. R.; Berthomieu, C.; Berger, G.; Nabedryk, E. *Biochemistry* **1994**, *33*, 4953−4965.
(23) Okamura, M. Y.; Isaacson, R. A.; Feher, G. *Proc. Natl. Acad. Sci. U.S.A.* **1975**, *72*, 3491−3495.
(24) Bauscher, M.; Nabedryk, E.; Bagely, K.; Mäntele, W. *FEBS Lett.* **1990**, *261*, 191−195.
(25) Burie, J.-R.; Boussac, A.; Boullais, C.; Berger, G.; Mattioli, T.; Mioskowski, C.; Nabedryk, E.; Breton, J. *J. Phys. Chem.* **1995**, *99*, 4059−4070.
(26) Knaff, D. B.; Malkin, R.; Myron, J. C.; Stoller, M. *Biochim. Biophys. Acta* **1977**, *459*, 402−411.
(27) Diner, B. A.; Vitry, C.; Popot, J.-L. *Biochim. Biophys. Acta* **1988**, *934*, 47−54.
(28) Noren, G. H.; Boerner, R. J.; Barry, B. A. *Biochemistry* **1991**, *30*, 3943−3950.
(29) Wise, K. E.; Grafton, A. K.; Wheeler, R. A. *J. Phys. Chem. A* **1997**, *101*, 1160−1165.
(30) Barry, B. A. *Methods Enzymol.* **1995**, *258*, 303−319.
(31) Steenhuis, J. J.; Barry, B. A. *J. Am. Chem. Soc.* **1996**, *118*, 11927−11932.
(32) Steenhuis, J. J.; Barry, B. A. *J. Phys. Chem. B* **1997**, *101*, 6652−6660.
(33) Steenhuis, J. J.; Barry, B. A. *J. Phys. Chem. B* **1998**, *102*, 4−8.
(34) Patzlaff, J. S.; Barry, B. A. *Biochemistry* **1996**, *35*, 7802−7811.
(35) Futami, A.; Hauska, G. *Biochim. Biophys. Acta* **1979**, *547*, 597−608.
(36) Becke, A. D. *J. Chem. Phys.* **1993**, *98*, 1372−1377.
(37) Scott, A. P.; Radom, L. *J. Phys. Chem.* **1996**, *100*, 16502−16513.
(38) Slater, J. C. *Quantum Theory of Molecules and Solids*; McGraw-Hill: New York, 1974; Vol. 4, pp 12−55.
(39) Becke, A. D. *Phys. Rev. A* **1988**, *38*, 3098−3100.
(40) Vosko, S. H.; Wilk, L.; Nusair, M. *Can. J. Phys.* **1980**, *58*, 1200−1211.
(41) Lee, C.; Yang, W.; Parr, R. G. *Phys. Rev. B* **1988**, *58*, 785−789.
(42) Hehre, W. J.; Radom, L.; Schleyer, P. v. R.; Pople, J. A. *Ab initio Molecular Orbital Theory*; John Wiley & Sons: New York, 1986.
(43) Helgaker, T.; Taylor, P. R. In *Modern Electronic Structure Theory*; Yarkony, D. R., Ed.; World Scientific: Singapore, 1995; Vol. 2, pp 725−856.
(44) Boesch, S. E.; Wheeler, R. A. *J. Phys. Chem.* **1995**, *99*, 8125−8134.
(45) Boesch, S. E.; Wheeler, R. A. *J. Phys. Chem. A* **1997**, *101*, 8351−8359.
(46) Boesch, S. E.; Wheeler, R. A. *J. Phys. Chem. A* **1997**, *101*, 5799−5804.
(47) Grafton, A. K.; Boesch, S. E.; Wheeler, R. A. *J. Mol. Struct. (THEOCHEM)* **1997**, *392*, 1−11.
(48) Grafton, A. K.; Wheeler, R. A. *J. Phys. Chem. A* **1997**, *101*, 7154−7166.
(49) Frisch, M. J.; Trucks, G. W.; Schlegel, H. B.; Gill, P. M. W.; Johnson, B. G.; Robb, M. A.; Cheeseman, J. R.; Keith, T.; Petersson, G. A.; Montgomery, J. A.; Raghavachari, K.; Al-Laham, M. A.; Zakrzewski, V. G.; Ortiz, J. V.; Foresman, J. B.; Cioslowski, J.; Stefanov, B. B.; Nanayakkara, A.; Challacombe, M.; Peng, C. Y.; Ayala, P. Y.; Chen, W.; Wong, M. W.; Andres, J. L.; Replogle, E. S.; Gomperts, R.; Martin, R. L.; Fox, D. J.; Binkley, J. S.; Defrees, D. J.; Baker, J.; Stewart, J. P.; Head-Gordon, M.; Gonzalez, C.; Pople, J. A. *GAUSSIAN 94*, revision B.2; Gaussian, Inc.: Pittsburgh, PA, 1995.
(50) Frisch, M. J.; Trucks, G. W.; Schlegel, H. B.; Scuseria, G. E.; Robb, M. A.; Cheeseman, J. R.; Zakrzewski, V. G.; Montgomery, J. A.; Strattman, R. E.; Burant, J. C.; Dapprich, S.; Millam, J. M.; Daniels, A. D.; Kudin, K. N.; Strain, M. C.; Farkas, O.; Tomasi, J.; Barone, V.; Cossi, M.; Cammi, R.; Menucci, C.; Pomelli, C.; Adamo, C.; Clifford, S.; Ochterski, J.; Petersson, G. A.; Ayala, P. Y.; Cui, Q.; Morokuma, K.; Malick, D. K.; Rabuck, A. D.; Raghavachari, K.; Foresman, J. B.; Cioslowski, J.; Ortiz, J. V.; Stefanov, B. B.; Liu, G.; Liashenko, A.; Piskorz, P.; Komaromi, I.; Gomperts, R.; Martin, R. L.; Fox, D. J.; Keith, T.; Al-Laham, M. A.; Peng, C. Y.; Nanayakkara, A.; Gonzalez, C.; Challacombe, M.; Gill, P. M. W.;

Johnson, B.; Chen, W.; Wong, M. W.; Andres, J. L.; Head-Gordon, M.; Replogle, E. S.; Pople, J. A. *GAUSSIAN98*, revision A.6; Gaussian, Inc: Pittsburgh, PA, 1998.

(51) Schlegel, H. B. *J. Comput. Chem.* **1986**, *3*, 214−218.

(52) Dupuis, M.; Spangler, D.; Wendoloski, J. J. *National Resource for Computations in Chemistry Software Catalog, Program QC01*; University of California: Berkeley, 1980.

(53) Schmidt, M. W.; Baldridge, K. K.; Boatz, J. A.; Jensen, J. H.; Koseki, S.; Gordon, M. S.; Nguyen, K. A.; Windus, T. L.; Elbert, S. T. *QCPE Bull.* **1990**, *10*, 52.

(54) Wasikowski, C.; Klemm, S. *XMOL*, version 1.3.1; In Research Equipment, Inc. d.b.a. Minnesota Supercomputer Center, Inc., 1993.

(55) Grafton, A. K.; Wheeler, R. A. *Comput. Phys. Commun.* **1998**, *113*, 78−84.

(56) Grafton, A. K.; Wheeler, R. A. *J. Comput. Chem.* **1998**, *19*, 1663−1674.

(57) Wise, K. E.; Pate, J. B.; Wheeler, R. A. *J. Phys. Chem. B* **1999**, *103*, 4764−4772.

(58) Zhao, X.; Imahori, H.; Zhan, C.-G.; Misutani, Y.; Sakata, Y.; Kitagawa, T. *Chem. Phys. Lett.* **1996**, *262*, 643−648.

(59) Bensasson, R.; Land, E. J. *Biochim. Biophys. Acta* **1973**, *325*, 175−181.

(60) MacDonald, G. M.; Boerner, R. J.; Everly, R. M.; Cramer, W. A.; Debus, R. J.; Barry, B. A. *Biochemistry* **1994**, *33*, 4393−4400.

(61) de Paula, J. C.; Innes, J. B.; Brudvig, G. W. *Biochemistry* **1985**, *24*, 8114−8120.

(62) de Paula, J. C.; Li, P. M.; Miller, A.-F.; Wu, B. W.; Brudvig, G. W. *Biochemistry* **1986**, *25*, 6487−6494.

(63) MacDonald, G. M.; Bixby, K. A.; Barry, B. A. *Proc. Natl. Acad. Sci. U.S.A.* **1993**, *90*, 11024−11028.

(64) Kim, S.; Liang, J.; Barry, B. A. *Proc. Natl. Acad. Sci. U.S.A.* **1997**, *94*, 14406−14412.

(65) Kim, S.; Barry, B. A. *Biochemistry* **1998**, *37*, 13882−13892.

(66) Kim, S.; Barry, B. A. *Biophys. J.* **1998**, *74*, 2588−2600.

(67) Ayala, I.; Kim, S.; Barry, B. A. *Biophys. J.* **1999**, *77*, 2137−2144.

(68) Berthomieu, C.; Nadedryk, E.; Mäntele, W.; Breton, J. *FEBS Lett.* **1990**, *269*, 363−367. Hienerwadel, R.; Boussac, A.; Breton, J.; Berthomieu, C. *Biochemistry* **1996**, *35*, 15447−15460. Zhang, H.; Razeghifard, M. R.; Fischer, G.; Wydrzynski, T. *Biochemistry* **1997**, *36*, 11762−11768.

(69) MacDonald, G. M.; Steenhuis, J. J.; Barry, B. A. *J. Biol. Chem.* **1995**, *270*, 8420−8428.

(70) Kruk, J.; Strzalka, K.; Leblanc, R. M. *Biophys. Chem.* **1992**, *45*, 161−169.

(71) Tripathi, G. N. R. *J. Chem. Phys.* **1981**, *74*, 6044−6049.

(72) Tripathi, G. N. R.; Schuler, R. H. *J. Phys. Chem.* **1987**, *91*, 5881−5885.

(73) Bauscher, M.; Leonhard, M.; Moss, D. A.; Mantele, W. *Biochim. Biophys. Acta* **1993**, *1183*, 59−71.

(74) Hanley, J.; Deligiannakis, Y.; Pascal, A.; Faller, P.; Rutherford, A. W. *Biochemistry* **1999**, *38*, 8189−8195.

(75) Rudiger, W.; Schoch, S. In *Chlorophylls*; Scheer, H., Ed.; CRC Press: Boca Raton, 1991; pp 451−464.

(76) Porra, R. J.; Klein, O.; Wright, P. E. *Eur. J. Biochem.* **1983**, *130*, 509−516.

(77) Nabedryk, E.; Leonhard, M.; Mantele, W.; Breton, J. *Biochemistry* **1990**, *29*, 3242−3247. Bellamy, L. J. *The infrared spectra of complex molecules*; Chapman and Hall: London, 1980; Vol. 1, pp 13−36, 203−220.

(78) Boldt, N. J.; Donohue, R. J.; Birge, R. R.; Bocian, D. F. *J. Am. Chem. Soc.* **1987**, *109*, 2284−2298. Fujiwara, M.; Tasumi, M. *J. Phys. Chem.* **1986**, *90*, 5646−5650.